Electronic Supplementary Information (ESI)

for

Dopamine-Derived Copper Nanocrystals as an Efficient Sensing, Catalysis and Antibacterial Agent

Hong Yan Zou,[ab] Jing Lan[a] and Cheng Zhi Huang*[ab]

[a] *Key Laboratory of Luminescence and Real-Time Analytical Chemistry (Southwest University), Ministry of Education, College of Pharmaceutical Sciences, Southwest University, Chongqing, 400715, P. R. China.*

[b] *College of Chemistry and Chemical Engineering, Southwest University, Chongqing, 400715, P. R. China.*

**Corresponding author: chengzhi@swu.edu.cn*

Quantum yield measurement

The quantum yield (QY) of CuNCs was measured according to an established procedure. Quinine sulfate in 0.1 M H_2SO_4 (literature quantum yield 0.54 at 360 nm) was chose as a standard. Absolute values are calculated using the standard reference sample that has a fixed and known fluorescence quantum yield value. To minimize reabsorption effects, absorbencies in the 10 mm fluorescence cuvette were kept under 0.1 at the excitation wavelength (320 nm). The data was plotted (Figure. S1) and the slopes of the sample and the standards were determined. The data showed good linearity. The quantum yield was calculated by

$$\Phi=\Phi_{st}\left(\frac{m_s}{m_{st}}\right)\left(\frac{\eta_s^2}{\eta_{st}^2}\right) \quad (1)$$

Where Φ is the quantum yield, m is slope, η is the refractive index of the solvent, st is the standard and s is the sample. The quantum yield for CuNCs was 9.6%.

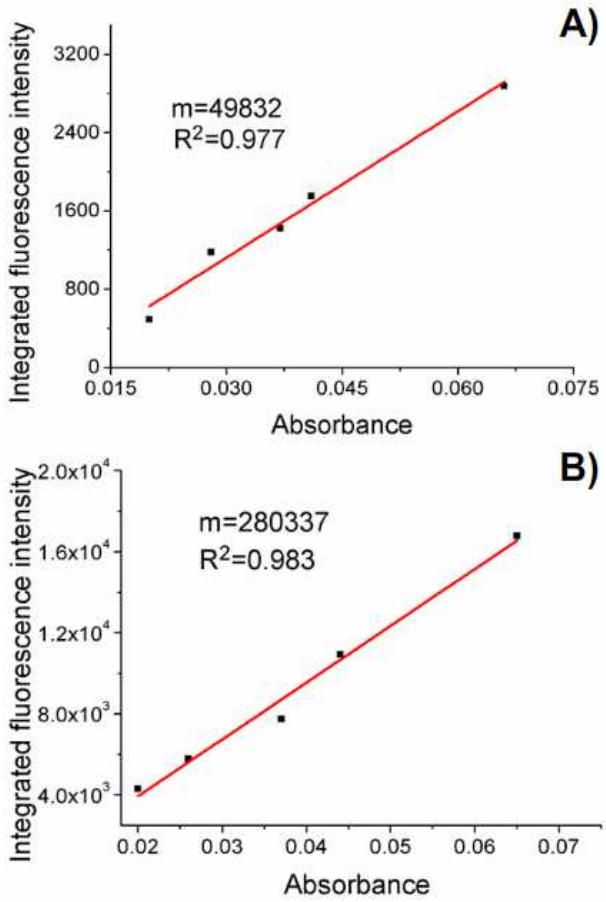

Figure S1 Plot of integrated photoluminescence intensity vs. absorbance of the small CuNCs (A) and quinine sulphate (B).

FL lifetimes measurement

The FL lifetimes was analysed with the software package, DataStation V2.4, and was fit by a sum of biexponential decay model,

$$F(t) = A_1 \exp(-\frac{t}{t_1} + A_2 \exp(-\frac{t}{t_2}) \quad (2)$$

Where F(t) is the obtained kinetic decay curve, A_i is the amplitude of the ith decay channel and τ_i is the corresponding lifetime. Two exponentials were required to fit the decay data, thus, the average lifetime (listed in Table S1) was calculated using

$$t = \frac{A_1 t_1 + A_2 t_2}{A_1 + A_2} \quad (3)$$

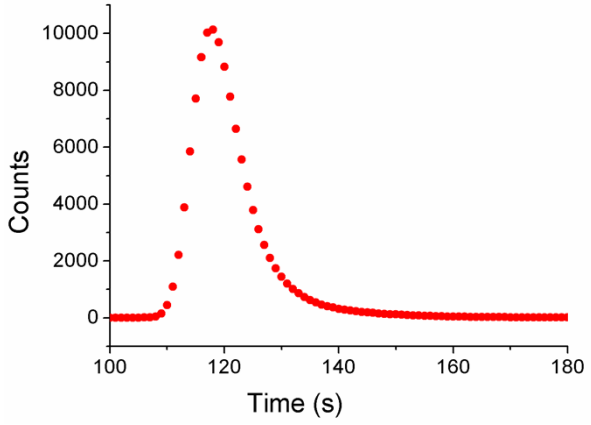

Figure S2 Time-resolved PL decays from the CuNCs.

Table S1 Excited State Lifetimes of the CuNCs

	Lifetime (ns)		
	τ_{av}	τ_1	τ_2
CuNCs	1.03	0.83	3.02
		(91.07%)	(8.93%)

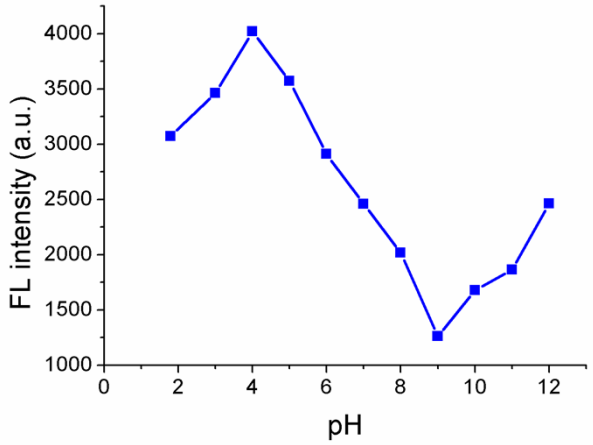

Figure S3 Effect of pH on the fluorescence intensity of small CuNCs (174 μg mL^{-1}).

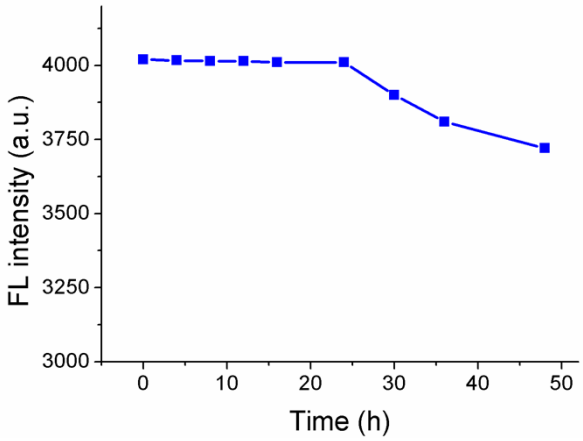

Figure S4 Effect of time on the fluorescence intensity of small CuNCs (174 μg mL^{-1}) at room temperature.

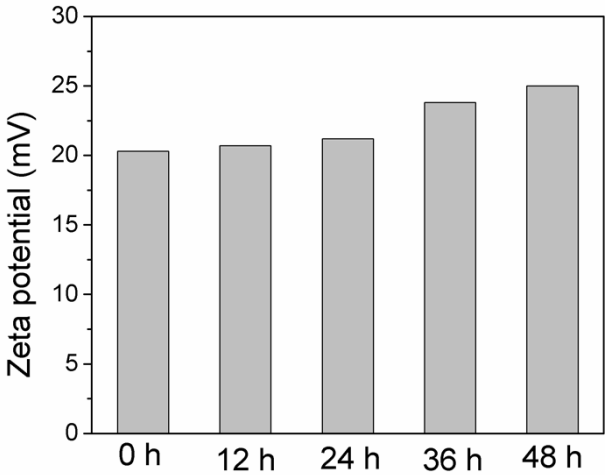

Figure S5 The zeta potential of small CuNCs (174 μg mL^{-1}, pH: 4, Dispersant RI: 1.330, Zeta runs: 30) at room temperature.

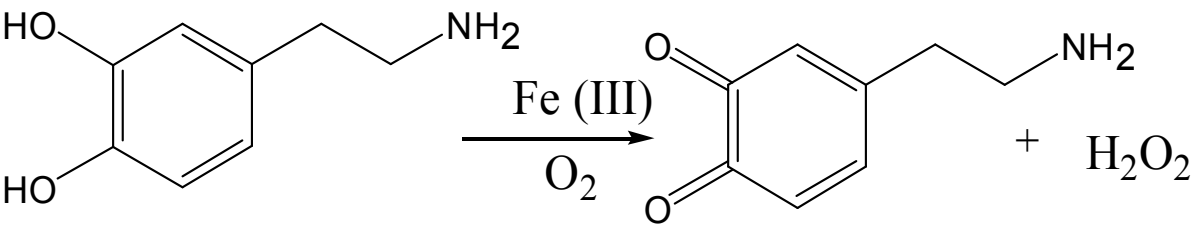

Scheme S1. The main proposed iron-induced DA oxidation pathway. In vitro, iron has

been shown to catalyse the oxidation of DA by oxygen to generate H_2O_2 and quinomethide.

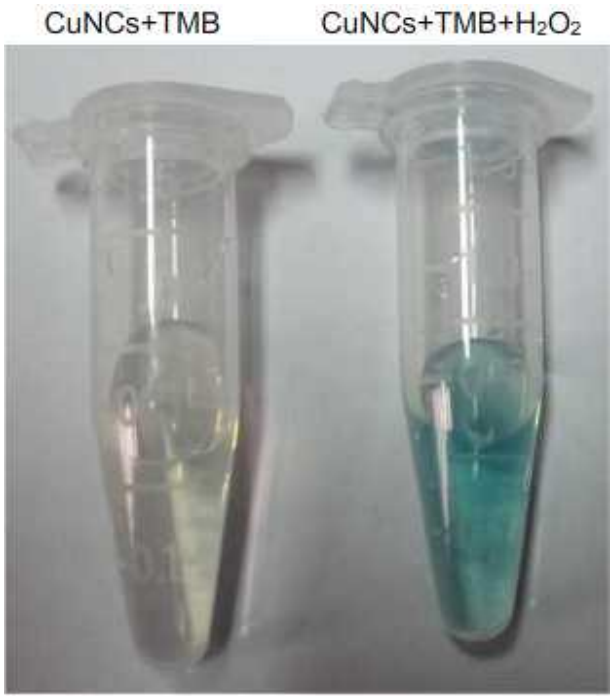

Figure S6 The oxidation of TMB (0.2 mM) in the absence (A) or presence (B) of H_2O_2 (10 mM) catalyzed by the small CuNCs (174 μg mL^{-1}).

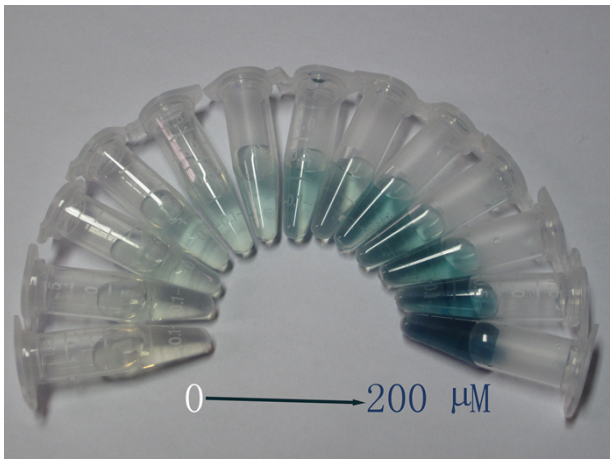

Figure S7 A gradient blue color which can be seen by naked eyes with increasing the

concentration of Fe^{3+} ions to the CuNCs (174 μg mL^{-1}) and TMB (0.2 mM) solution.

Detection of Fe^{3+} in tap water and lake water

The lake water sample was obtained from a local lake and filtered five using the filter paper to remove the solid suspensions and then filtered through a 0.22 μm membrane and then centrifuged at 10000 rpm for 10 min several times. The resultant water samples were add with Fe^{3+} and then analysed with the proposed method.

Reactive Oxygen Species (ROS) Assays

The ability of surface modified CuNCs to generate ROS in solution was measured using a fluorescent dye (2, 7-dichlorodihydroflurescein diacetate, DCFH-DA) and a spectrofluorometer (absorbance maximum, 485 nm; emission maximum, 535 nm). The non-fluorescent molecule DCFH-DA (0.5 mL, 1.23 mM) was deacetylated in a solution using NaOH (2 mL, 0.01M) and the mixture was incubated at room temperature in a dark bottle for 30 min. Then 2 mL of BR buffer (0.2 M, pH=7.0) was added to stop the reaction. Right before use, 100 μL horseradish peroxidase (HRP) in BR buffer was added to 100 μL DCFH-DA /NaOH/BR. H_2O_2 (5.28, 7.04, 8.8, 10.56, 12.32 μM) was used as a standard and CuNCs activity was expressed in H_2O_2 equivalents. The final solution was 1 mL in volume in a water bath in the dark at 37 °C for 15 min.

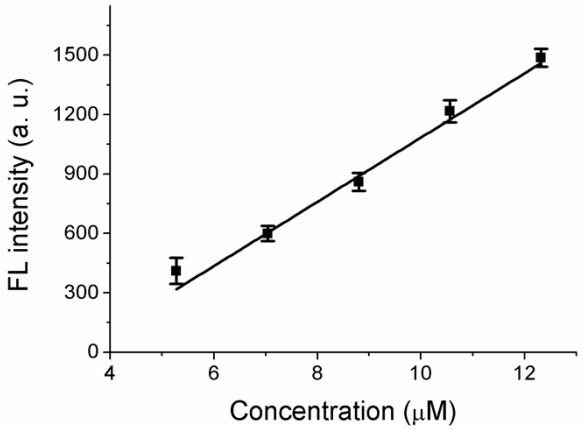

Figure S8 H_2O_2 calibration curve by the DCFH Assay.

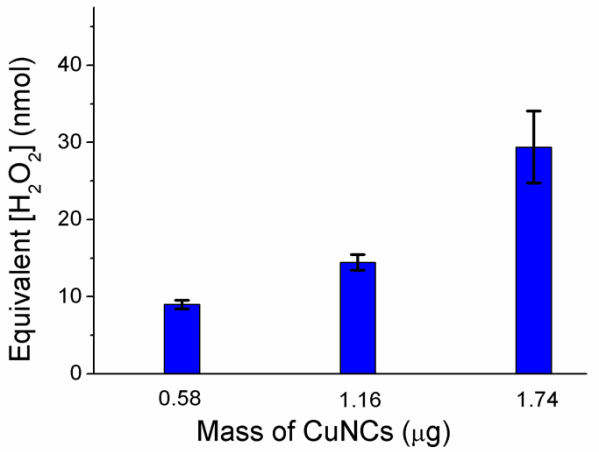

Figure S9 Equivalent H_2O_2 generated by CuNCs.

Table S2 Literature review of copper clusters or nanoparticles used as sensing nanoprobes.

Sample	Protecting ligand or method	Ion Detected	Mechanism	Linear range	Ref.
Copper clusters	Tannic acid	Fe^{3+}	FL quenching	10 nM–10 mM LOD=10 nM	1
Copper clusters	BSA	Pb^{2+}	FL quenching	0–200 ppm	2
Copper clusters	Electrochemically method	Pb^{2+}	FL quenching	48 nM–77 mM LOD=4.9 mM	3
Copper nanoparticles	CTAB	S^{2-}	Colorimetric sensing	12.5–50.0 μM LOD=8.1 μM	4
Copper Nanoparticles	dsDNA	Alkaline Phosphatase	FL turn-on	0.1–2.5 nM LOD= 0.1 nM	5
Copper clusters	D-penicillamine	pH, H_2O_2	FL quenching	pH 3.1–7.1 H_2O_2 0.01–0.8 mM LOD=0.01 mM	6
Copper clusters	Trypsin	pH	FL quenching	pH 2.02–12.14	7
Copper nanoparticles	dsDNAs	Hg^{2+}	FL turn-on	/	8
Copper nanocrystals	Dopamine	Fe^{3+}	FL quenching Colorimetric sensing	5 –300 μM LOD=1.2 μM; 10–80 μM LOD=4.2 μM	Our work

Table S3 Literature review of copper clusters or nanoparticles used for catalytic applications.

Samples	Protecting ligand or method	catalytic applications	Mechanism	Ref.
Copper clusters	D-penicillamine	MB-N_2H_4	Electron transfer	6
Copper clusters	Electrochemical method	MB-N_2H_4	Electron transfer	9
Copper clusters	Electrochemical method	MB	Photocatalysis and Electron transfer	10
Copper clusters	BSA	TMB- H_2O_2	Peroxidase mimetics	11
Copper nanocrystals	Dopamine	TMB	Peroxidase mimetics and chemical reactions	Our work

Table S4 Literature review of copper clusters or nanoparticles used as antibacterial agent.

Samples	Bacteria	MIC	Mechanism	Ref.
copper monodispersed nanoparticles into sepiolite	*S. aureus* *E. coli*	/	Metallic copper in solution	12
Cu Nanoparticle Chitosan Composite	*E. coli*	130.8 μg/mL	Nanocomposite attached to the bacterial cell wall	13
BSA-copper nanocomposites	*E. coli*	50 μg/mL	Cu-BSA attached to the bacteria causing irreversible membrane damage	14
Cu/PAA composite	*S. aureus* *E. coli* *P. aeruginosa*	2.34 μg/mL 0.59 μg/mL 0.59 μg/mL	Cu ions release	15
Copper nanocrystals	*S. aureus*	158 μg/mL	Reactive oxygen species	Our work

Optimization process

CuNCs were prepared by various molar ratio of DA to copper salt (1:3, 1:2, 1:1, 2:1,

3:1) using the same method described in the main text.

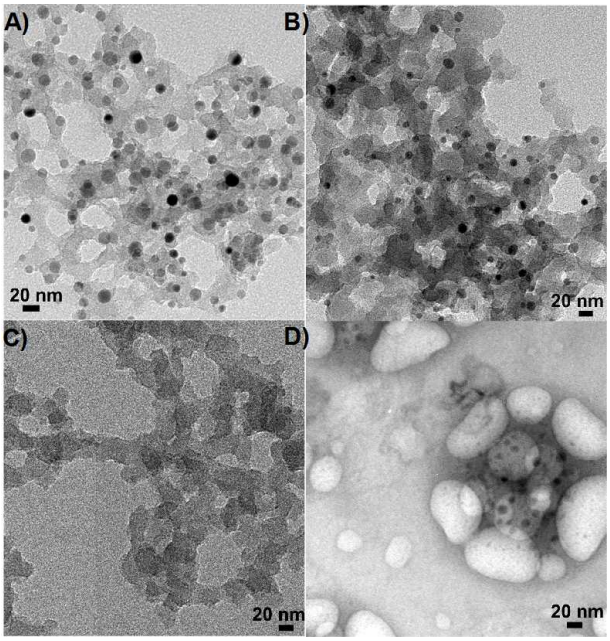

Figure S10 TEM image of CuNCs synthesized by various molar ratio of DA to copper salt (A: 1:3, B: 1:2, C: 2:1, D: 3:1).

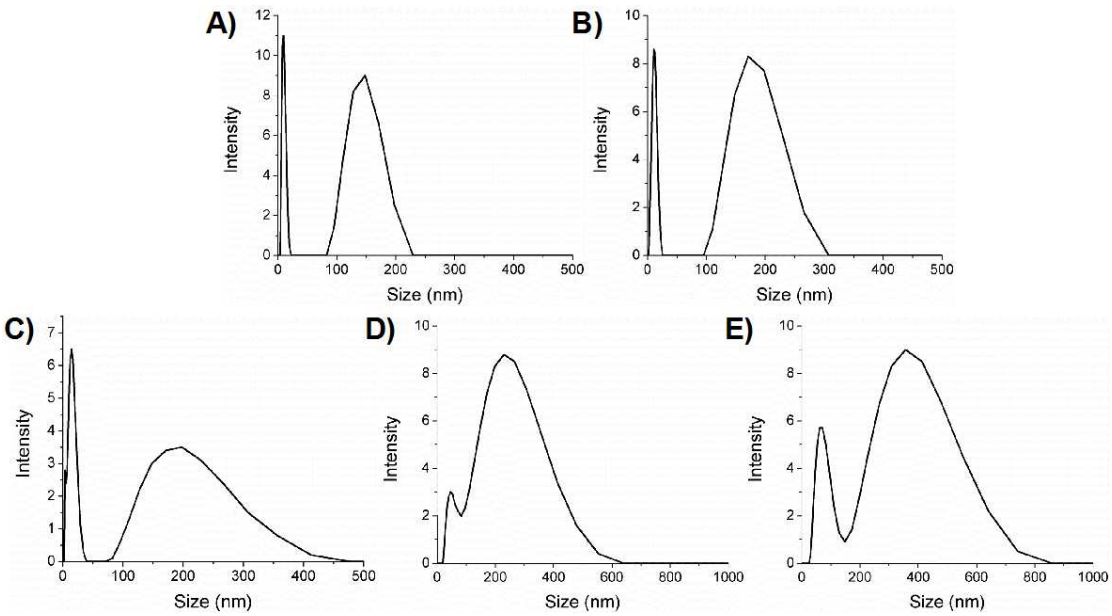

Figure S11 Hydrodynamic diameter of CuNCs synthesized (174 μg mL^{-1}, pH: 4, Dispersant RI: 1.330) by various molar ratio of DA to copper salt (A: 1:3, B: 1:2, C:

1:1, D: 2:1, E: 3:1).

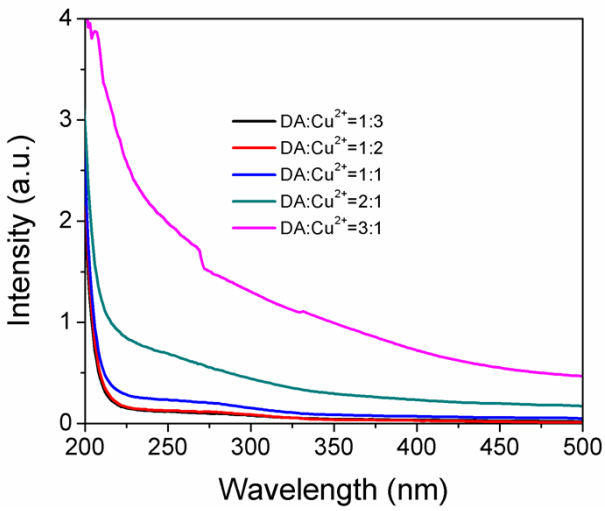

Figure S12 UV-vis spetra of CuNCs (174 μg mL^{-1}) synthesized by various molar ratio of DA to copper salt (1:3, 1:2, 1:1, 2:1, 3:1).

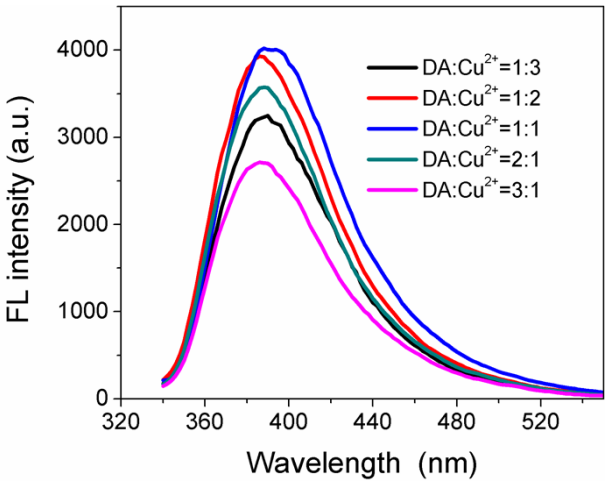

Figure S13 FL spetra of CuNCs (174 μg mL^{-1}) synthesized by various molar ratio of DA to copper salt (1:3, 1:2, 1:1, 2:1, 3:1).

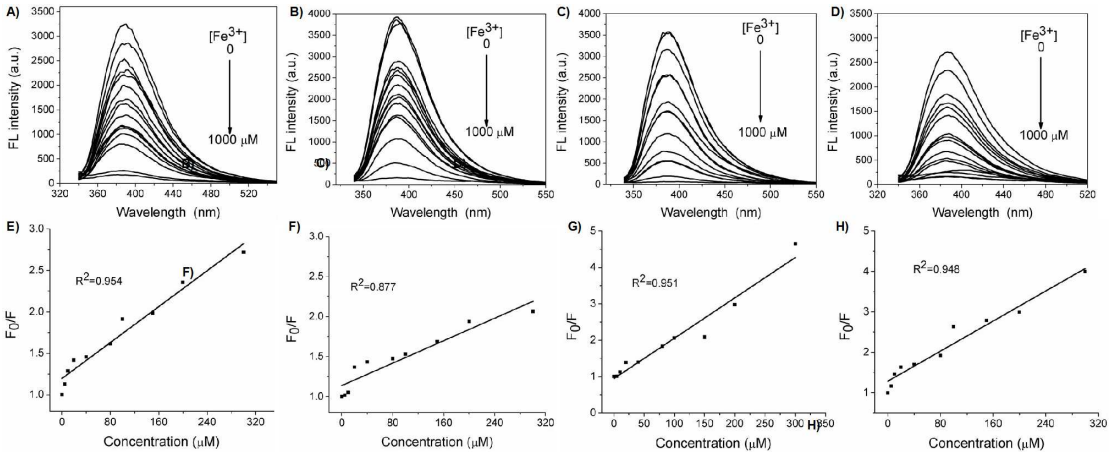

Figure S14 (A-D) Fluorescence spectra of obtained CuNCs synthesized by various molar ratio of DA to copper salt (174 μg mL^{-1}, A: 1:3, B: 1:2, C: 2:1, D: 3:1) in the presence of Fe^{3+} ions with different concentrations (0, 5, 10, 20, 40, 80, 100, 150, 200, 300, 400, 500, 600, 700, 800, 1000 μM). (E-H) Calibration curve (E: 1:3, F: 1:2, G: 2:1, H: 3:1) for Fe^{3+} ions detection by fluorescence intensities (F_0/F).

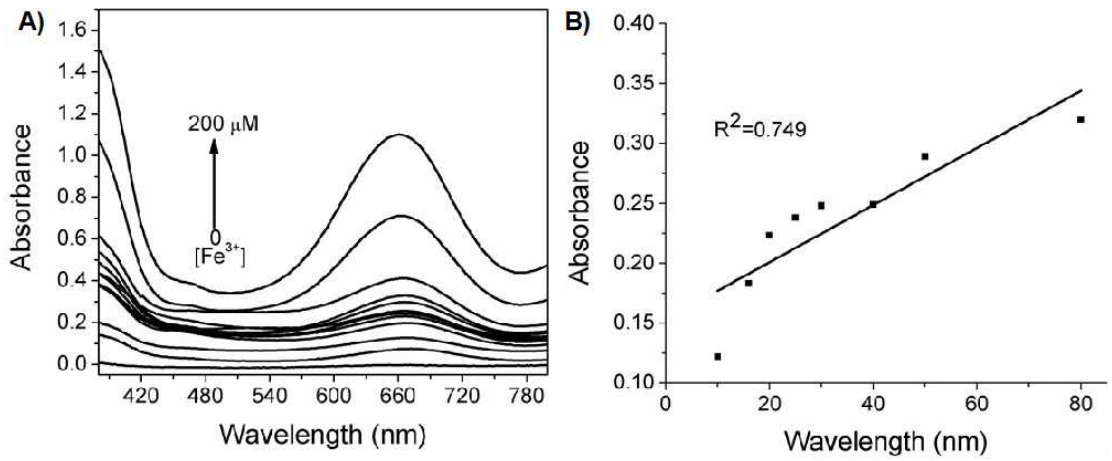

Figure S15 A) UV-vis absorption of the oxidation product of TMB with increasing Fe^{3+} concentrations (0, 6, 10, 16, 20, 25, 30, 40, 50, 80, 100, 160, 200 μM) with Cu nanoparticles (174 μg mL^{-1}) prepared by ref.16 (B) Calibration curve for Fe^{3+} ions (10 –80μM) detection by absorbance using the peroxidase-like activity of Cu nanoparticles.

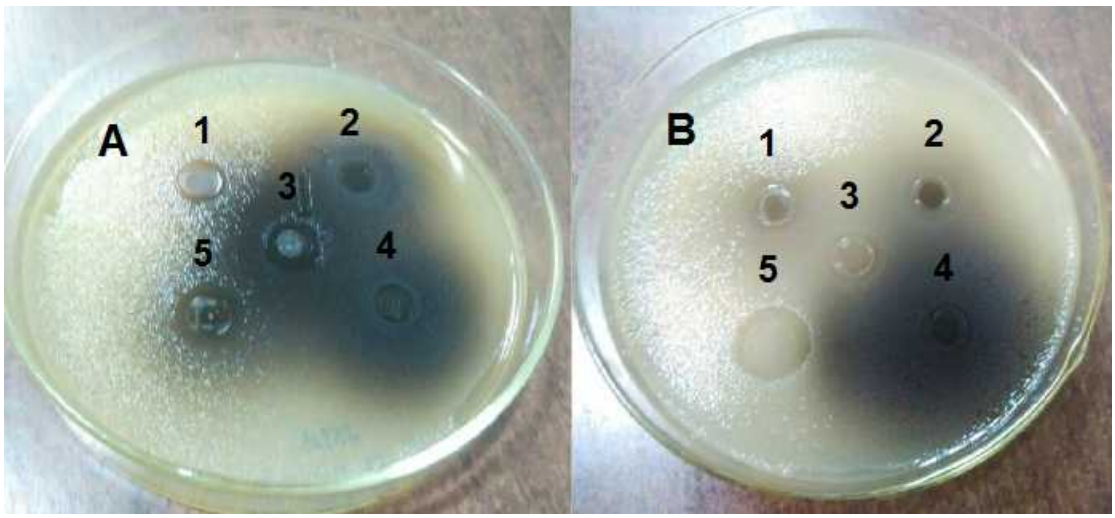

Figure S16 Growth inhibition of S. *aureus* bacteria on agar plate for different samples. (A) The antimicrobial activity shown with CuNCs (174 μg mL^{-1}) synthesized by various molar ratio of DA to copper salt. Spots 1-5 represent the ratio 1:3, 1:2, 1:1, 2:1, 3:1. (B) Separate experiments for evaluating the antimicrobial activity with 174 μg mL^{-1} CuNCs (spot 1), 174 μg mL^{-1} Cu nanoparticles prepared by ref.16 (spot 2), 0.02 M $CuSO_4$ (spot 3), 0.06 M dopamine (spot 4) and174 μg mL^{-1} Ag cluster prepared by ref.17(spot 5).

References

1 H. Y. Cao, Z. H. Chen, H. Z. Zheng and Y. M. Huang, *Biosen.Bioelectron*., 2014, **62**, 189–195.
2 N. Goswami, A.Giri, M. S. Bootharaju, P.Lourdu Xavier, T. Pradeep and S. Kumar Pal, *Anal. Chem*., 2011, **83**, 9676–9680.
3 N. Vilar-Vidal, J. Rivas and M. A. López-Quintela, *Phys. Chem. Chem. Phys*., 2014,**16**, 26427–26430.
4 A. Hatamie, B. Zargar, A. Jalali, *Talanta*, 2014, **121**, 234–238.
5 L. I. Zhang, J. J. Zhao, M. Duan, H. Zhang, J. H. Jiang and R. Q. Yu, *Anal. Chem*., 2013, **85**, 3797−3801.
6 X. F. Jia, X.Yang, J. Li, D. Y. Li, E. Wang, *Chem. Commun*., 2014, **50**, 237–239.
7 W. Wang, F. Leng, L. Zhan, Y. Chang, X. X.Yang, J. Lan and C. Z. Huang, *Analyst*, 2014, **139** , 2990–2993.
8 G. Y. Liu, Y. Shao, J. Peng, W. Dai, L. L. Liu, S. J. Xu, F. Wu and X. H. Wu, Nanotechnology, 2013, **24**, 345502.
9 N. Vilar-Vidal, J. Rivas and M. A. López-Quintela, *ACS Catal*. 2012, **2**, 1693−1697.
10 N. Vilar-Vidal, J. Rivas and M. A. López-Quintela, *Small,* 2014, **10***,* 3632–3636.
11 L. Hu, Y. Yuan, L. Zhang, J. Zhao, S. Majeed, and G. Xu, *Anal Chim Acta*., 2013. **762**, 83–86.

12 A. Esteban-Cubillo, C Pecharroman, E. Aguilar, J. Santaren and J. S. Moya, *J. Mater. Sci.*, 2006, **41**, 5208−5212.
13 S. Mallick, S. Sharma, M. Banerjee, S. S. Ghosh, A. Chattopadhyay and A. Paul, *ACS Appl. Mater. Interfaces,* 2012, **4**, 1313–1323.
14 L. Rastogi and J. Arunachalam, *Colloid Surf. B-Biointerfaces*, 2013, **108**, 134–141.
15 B.J. Li , Y. Y. Li, Y. H. Wu and Y. B. Zhao, *Mater. Sci. Eng. C*, 2014, 35, 205–211.
16 J. Xiong, X. D. Wu and Q. J. Xue, *J. Colloid Interface Sci*., 2013, **390**, 41–46.
17 J. Lan, P. Zhang, T. T. Wang, Y. Chang, S. Q. Lie, Z. L. Wu, Z. D. Liu, Y. F. Li and C. Z. Huang, *Analyst*, 2014, **139**, 3441−3445.